J. Meas. Sci. Instrum., 2025, 16(3): 456-463. http://jmsi.publish.founderss.cn
DOI: 10.62756/jmsi.1674-8042.2025044 jmsi@nuc.edu.cn

Fault diagnosis of three-phase inverter based on GAF-CNN

DONG Weiguang, LU Haobo*, LI Shengchang

School of Automation and Electrical Engineering, Lanzhou Jiaotong University, Lanzhou 730070, China

***Corresponding author:** LU Haobo (11200373@stu.lzjtu.edu.cn)

Received: January 2, 2024 **Revised:** January 19, 2024 **Accepted:** January 22, 2024

Abstract: To apply the advantages of deep learning in recognizing two-dimensional (2D) images to three-phase inverter fault diagnosis, a three-phase inverter fault diagnosis model based on gramian angular field (GAF) combined with convolutional neural network (CNN) was proposed. Since the current signals of the inverter in different working states are different, the images formed by the time series encoding are also different, which enables the image recognition technology to be used for time series classification to identify the fault current signal of the inverter. Firstly, the one-dimensional (1D) inverter fault current signal was converted into a 2D image through the GAF. Next, the CNN model suitable for inverter fault diagnosis was input to realize the detection, classification and location of inverter fault. The simulation results show that the recognition accuracy of this method is 99.36% under different noisy data. Compared with other traditional methods, it has higher accuracy and reliability, and stronger anti-noise interference capability and robustness in dealing with noisy data. Therefore, it is an effective fault diagnosis method for inverters.

Key words: fault diagnosis; gramian angular field (GAF); convolutional neural network (CNN); anti-noise interference; robustness

0 Introduction

As an emerging discipline and a very important branch in the field of new energy power, power electronics technology has made great development in recent years. Three-phase voltage source inverter is widely studied and applied in various important fields[1-3]. The main electrical circuit of the inverter is composed of several insulated gate bipolar transistors (IGBT). The high-frequency disconnection of IGBT makes the inverter prone to fault, which is generally divided into short-circuit fault and open circuit fault[4]. In case of short-circuit fault, the inverter starts the short-circuit protection device to cut off the switch tube, which is converted to open-circuit fault[5]. Therefore, correct fault diagnosis strategy and accurate fault separation technology have also become important means to improve the reliability of inverter system[6]. At present, there are three main types of inverter fault diagnosis methods, which are based on signal, model and knowledge, respectively[7]. The diagnostic method based on signal processing realizes fault diagnosis by analyzing the output current or voltage signal of the inverter[8,9]. This method is simple and easy to implement, but the real-time performance of diagnosis is poor in specific application. The model-based method is to build a mathematical model of the inverter and obtain the residual signal to achieve fault detection[10]. The accuracy of this method depends on the accuracy of the mathematical model built. The knowledge-based diagnostic method is to detect fault through the knowledge base and the processing power of the computer[11]. Convolutional neural network (CNN) has obvious advantages over shallow models in feature extraction and modeling[12-14]. Both 1D signals and 2D images can be used as the input of CNN, and the 2D image input method has higher accuracy and robustness than the 1D signal input method[15-18].

In summary, this paper presents a method that combines gramian angular field (GAF) and CNN, converts the open-circuit fault signal of the inverter into a 2D image through GAF. Furthermore, based on the established CNN model, the hidden features of the 2D image are extracted to realize the fault detection, classification and localization of the inverter.

1 GAF

GAF can encode the original 1D time series into a 2D image with more concentrated features[19].

First, GAF scales the original 1D time series $\boldsymbol{X}=\{x_1,x_2,\cdots,x_i,\cdots,x_n\}$ into a time series $\tilde{\boldsymbol{X}}_i$ on the interval $[-1, 1]$ as $\tilde{\boldsymbol{X}}_i=\{\tilde{x}_1,\tilde{x}_2,\cdots,\tilde{x}_i,\cdots,\tilde{x}_n\}$. The scaling conversion formula is

$$\tilde{x}_i=\frac{\left[x_i-\max(\boldsymbol{X})\right]+\left[x_i-\min(\boldsymbol{X})\right]}{\max(\boldsymbol{X})-\min(\boldsymbol{X})},\tag{1}$$

where 1D time series consists of n time stamps t with equal span and corresponding measurement data x.

Then, the value of the scaled 1D time series $\tilde{\boldsymbol{X}}_i$ is mapped to angle and converted to θ_i, and the time is mapped to r_i, and the time series in polar coordinates is obtained after conversion. The formula for converting a 1D time series$\tilde{\boldsymbol{X}}_i$ to a time series $\tilde{\boldsymbol{X}}$ on polar coordinates is

$$\begin{cases}\theta_i=\arccos\tilde{x}_i, & -1\leqslant\tilde{x}_i\leqslant 1,\ \tilde{x}_i\in\tilde{\boldsymbol{X}}_i,\\ r_i=\dfrac{t_i}{N}, & t_i\in N,\end{cases}\tag{2}$$

where N is a constant as a regularization factor for polar space.

The above transformation has two characteristics: 1) Because the cos θ is monotonically decreasing when it is on $\theta\in[0,\pi]$, the points in the 1D time series and the polar coordinate series are in one-to-one correspondence, that is, bijective; and 2) Polar coordinates have an absolute time relationship. Moreover, the time series within the interval $[-1,1]$ are converted into that on polar coordinates within the angle range of $[0,\pi]$.

After the 1D time series is transformed into the polar coordinate system by Eqs. (1) and (2), by calculating the difference of trigonometric function between each two points, the angle perspective is used to identify the difference between different time correlation. GAF is defined as

$$\boldsymbol{G}_{\mathrm{D}}=\begin{bmatrix}\sin(\theta_1+\theta_1) & \cdots & \sin(\theta_1+\theta_n)\\ \sin(\theta_2+\theta_1) & \cdots & \sin(\theta_2+\theta_n)\\ \vdots & & \vdots\\ \sin(\theta_n+\theta_1) & \cdots & \sin(\theta_n+\theta_n)\end{bmatrix}=\sqrt{\boldsymbol{I}-\tilde{\boldsymbol{X}}^2}^{\mathrm{T}}\tilde{\boldsymbol{X}}-\tilde{\boldsymbol{X}}^{\mathrm{T}}\sqrt{\boldsymbol{I}-\tilde{\boldsymbol{X}}^2},\tag{3}$$

where $\boldsymbol{I}$ is the unit row vector, and the gram matrix encodes the time information of the sequence from the upper left corner to the lower right corner, strictly maintaining the time dependence of the signal.

To sum up, GAF is an effective means to solve the problem that 1D time series cannot explain the underlying state and information of signals to some extent.

2 CNN

2.1 Structure of CNN

A standard CNN generally consists of an input layer, alternating convolutional layer and pooling layer, a fully connected layer, and an output layer[20].

The input layer inputs a 2D feature map or a raw data map. Unlike other networks, CNN does not require vectorized input data. The input layer is used as the data input port of the neural network, and the number of neurons should be consistent with the number of image pixels generated by the GAF.

Fig. 1 shows the basic structure of the convolutional layer. The convolutional layer traverses each pixel on the image through the convolutional kernel, performs convolutional operations on different areas on the image, and then extracts the hidden features of the input image through the activation function. The operation formula is

$$x_j^l=f\left(\sum_{I\in M_j}X_I^{l-1}*k_{ij}^l+b_j^i\right),\tag{4}$$

where f is the nonlinear activation function, l is the lth layer in the network model, x_j^l is the jth feature image in the lth layer, k_{ij}^l is the weight of the convolutional kernel; b_j^i is the offset required for the operation, M_j is the 2D image dataset of the input model, and * represents the convolutional operation.

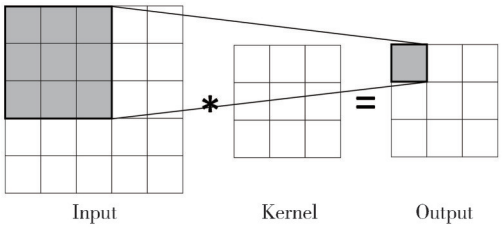

Fig. 1 Basic structure of convolutional layer

Since ReLU function has a faster convergence speed than tanh and Sigmod functions, it is used to solve the problem of gradient dispersion. The ReLU function is defined as

$$f_{\mathrm{ReLU}}(x)=\max(0,x).\tag{5}$$

To set the hyperparameters of the network more freely, such as larger learning rate, more random network initialization, etc., while making the network get faster convergence speed and better performance, we add a batch nomalization (BN) layer between the convolutional layer and the ReLU function. The input of BN layer is $x_i\in\{x_1,x_2,\cdots,x_{\mathrm{m}}\}$, and the output is the normalized network response $y_i=y_{\gamma,\beta}^{\mathrm{BN}}(x_i)$. The BN layer process is as follows.

1) Obtaining the mean of each training batch by

$$\mu_{\mathrm{B}}=\frac{1}{m}\sum_{i=1}^{m}x_i.\tag{6}$$

2) Obtaining the variance of each training batch by

$$\sigma_{\mathrm{B}}^2=\frac{1}{m}\sum_{i=1}^{m}\left(x_i-\mu_{\mathrm{B}}\right)^2.\tag{7}$$

3) Normalizing the batch of training data using the obtained mean and variance to obtain a 0—1 distribution as

$$\hat{x}_i = \frac{x_i - \mu_{\mathrm{B}}}{\sqrt{\sigma_{\mathrm{B}}^2 + \varepsilon}}, \tag{8}$$

where ε is a tiny positive number to avoid division by 0.

4) Scaling and obtaining the offset y_i by multiplying x_i by γ to adjust the value and then adding β as

$$y_i = \gamma \hat{x}_i + \beta = y_{\gamma,\beta}^{\mathrm{BN}}(x_i), \tag{9}$$

where γ is the scale factor, and β is the translation factor, which are obtained as parameters to be learnt when training the network.

Fig.2 shows the basic structure of the pooling layer. The pooling layer is to obtain new element values by sampling or aggregating information from a set of locally related elements, which reduces the data dimension processed by the convolutional layer and removes redundant information by compressing features, thus simplifying network complexity degree, and reducing the amount of calculation and memory consumption.

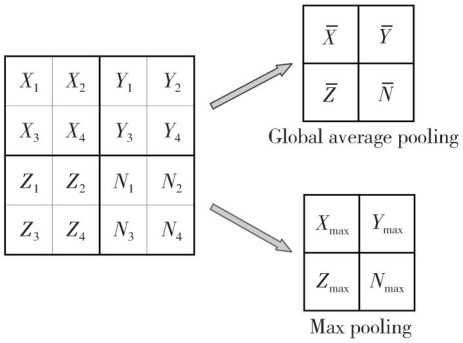

Fig. 2 Basic structure of pool layer

There are two common pooling methods, max pooling and global average pooling, which are defined as

$$y^{(l)} = \max\left[x_{ij}^{(l)}\right], \tag{10}$$

$$y^{(l)} = \frac{1}{m \times n}\left[\sum_{i=0}^{m}\sum_{j=0}^{m} x_{ij}^{(l)}\right], \tag{11}$$

where $m \times n$ is the size of the feature map of the last convolutional layer, with the value of the nth feature map represented by $x_{ij}^{(l)}$, and $y^{(l)}$ is the output of the pooling layer, with the combination of all outputs in the pooling layer as the final output of the pooling layer.

The fully connected layer integrates the class-discriminative feature information in the convolutional layer and the pooling layer, and then is output to the classifier. The output layer shows the final classification result in the form of probability. The number of neurons is consistent with the type of faults to be identified. Generally, the Softmax function is used for feature classification. It maps the output value to the interval of [0, 1] to make the sum of all output values to be 1, thus transforming it into a probability problem for multi-classification. The Softmax function is defined as

$$\boldsymbol{h}_\theta(x_i) = \begin{bmatrix} p(y_i = 1 | x_i; \boldsymbol{\theta}) \\ p(y_i = 2 | x_i; \boldsymbol{\theta}) \\ \vdots \\ p(y_i = k | x_i; \boldsymbol{\theta}) \end{bmatrix} = \frac{1}{\sum_{j=1}^{k} \mathrm{e}^{\theta_j^{\mathrm{T}} x_i}} \begin{bmatrix} \mathrm{e}^{\theta_1^{\mathrm{T}} x_i} \\ \mathrm{e}^{\theta_2^{\mathrm{T}} x_i} \\ \vdots \\ \mathrm{e}^{\theta_k^{\mathrm{T}} x_i} \end{bmatrix}, \tag{12}$$

where $p(y_i = k)$ is the probability output by the Softmax layer, with the value is in the range of [0, 1], $\boldsymbol{\theta}$ is the parameter of the Softmax classifier, $1 \Big/ \left(\sum_{j=1}^{k} \mathrm{e}^{\theta_j^{\mathrm{T}} x_i}\right)$ represents the probability normalization of the output, that is, the total probability of the output is 1.

2.2 CNN model

The CNN model in our work consists of input layer, three alternating layers of convolutional layer+max pooling layer, one layer of convolution layer+global average pooling layer and fully connected layer+Softmax classifier.

The structure of the CNN model is shown in Fig.3.

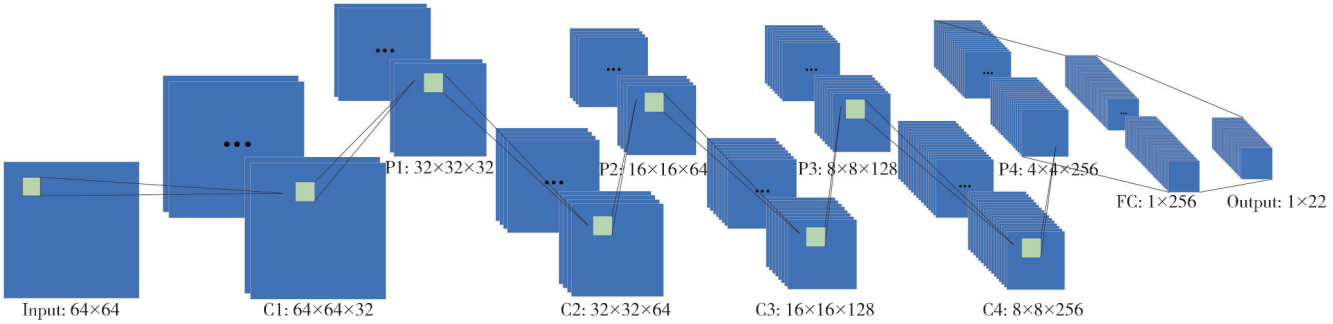

Fig. 3 Structure model of CNN

Table 1 lists the parameters of each layer of the network, where Padding= "same" means that the original image will be automatically filled with all 0 s. When the step size of the convolutional layer is 1, the output image can be guaranteed to be the same size as the input image.

Table 1 Results of state recognition

No.	Type	Kernel size	Quantity	Step size	Remark
1	Convolutional	3×3×3	32	1	Padding="same"
2	Max pooling	2×2	32	2	/
3	Convolutional	3×3×3	64	1	Padding="same"
4	Max pooling	2×2	64	2	/
5	Convolutional	3×3×3	128	1	Padding="same"
6	Max pooling	2×2	128	2	/
7	Convolutional	3×3×3	256	1	Padding="same"
8	Global average pooling	2×2	256	2	/
9	Fully connected layer	22	1	/	/

3 Fault diagnosis based on GAF-CNN

The fault diagnosis process based on GAF-CNN is descrided as follows.

1) Collecting fault signals from the circuit model.

2) Dividing the collected fault signals according to the period of current change, with one cycle of 0.02 s.

3) Converting the divided fault signals into the 2D image via GAF encoding.

4) Inputting the obtained image into the built CNN model, extracting the features in the image, and getting the information about different types of faults.

5) Classifying the faults by Softmax classifier to obtain the final results.

Fig. 4 is a block diagram of the GAF-CNN fault diagnosis method.

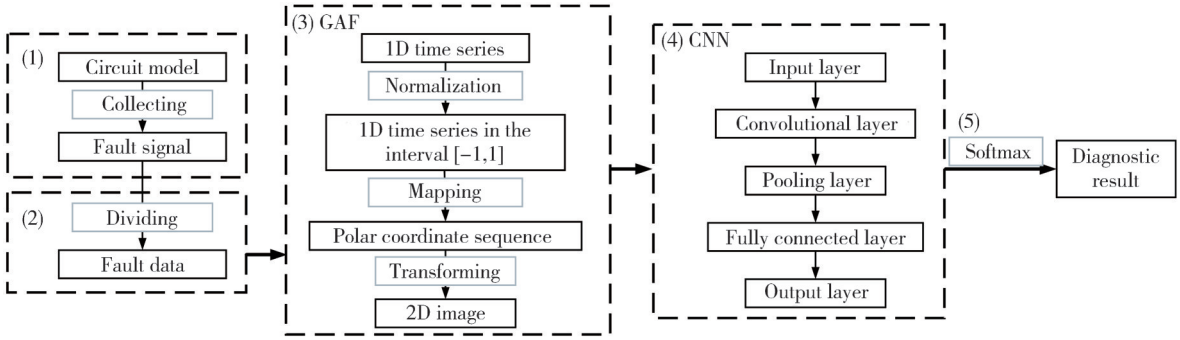

Fig. 4 Block diagram of GAF-CNN fault diagnosis method

4 Simulation and analysis

4.1 Inverter model

Considering that CNN needs a lot of data in the training process, a three-phase voltage source inverter model was established in Matlab/Simulink to obtain the current data of the inverter under different working states. The inverter topology is shown in Fig.5.

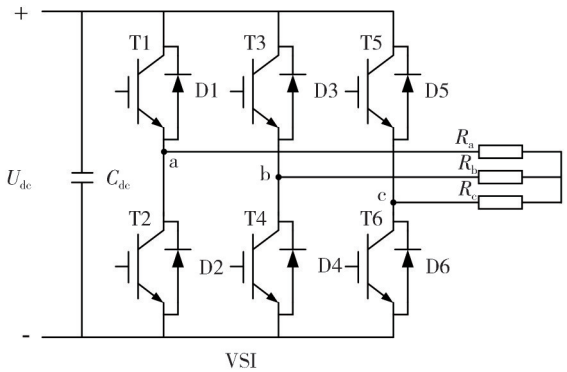

Fig. 5 Circuit topology diagram of voltage source inverter

The main circuit of the voltage source inverter consists of six bridge arms. The basic working mode of the voltage source inverter is a 180° conduction mode. The upper and lower arms of the same half-bridge are alternately conductive, and the angle difference between the conduction angles of each phase is 120°. In an instant, three bridge arms are turned on at the same time. Each commutation is performed between the upper and lower arms of the same phase, also known as longitudinal commutation.

The three-phase inverter has 1 normal working condition and 21 open-circuit fault conditions, totaling 22 working states. Among them, the open-circuit fault is divided into single-tube fault and double-tube fault. Furthermore, the double-tube fault is divided into two-IGBT fault in the same phase bridge arm, two-IGBT fault in the same half bridge, and two-IGBT fault in the cross bridge arm. The fault types are shown in Table 2.

Table 2 Fault type of inverters

Fault No.	Fault power tube	Fault type
C_1	None	Normal
C_2	T1, T2, T3, T4, T5, T6	Single IGBT fault
C_3	T1, T2, T3, T4, T5, T6	Two-IGBT fault in the same phase bridge arm
C_4	T1T3, T1T5, T3T5, T2T4, T2T6, T4T6	Two-IGBT fault in the same half bridge
C_5	T1T4, T1T6, T2T3, T2T5, T3T6, T4T5	Two-IGBT fault in cross bridge arm

4.2 Conversion of 1D time series to 2D image

When T_1 tube has an open-circuit fault and $I_a<0$, the A-

phase current flows through only T_1 or D_2, the current is not affected. When $I_a>0$, the A-phase current flows through only D_2, and D_2 continues to flow normally, but the A-phase current will be affected by the disconnection of T_1 and does not increase in the positive direction. Here, we select the current waveform data of a complete cycle after the fault , that is, a 1D fault time series, and convert it into a 2D GAF image. Fig.6 is the current waveform of phase A and the converted GAF image when T_1 tube has an open-circuit fault at 0.20 s.

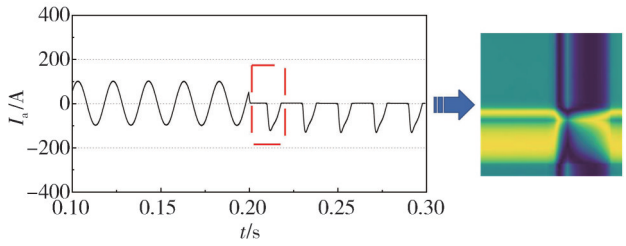

Fig. 6 A-phase current waveform and GAF image of T_1 tube open-circuit fault

When T_1 and T_2 tubes have an open-circuit fault, the path of A-phase current is blocked, and thus the A-phase current is 0. Fig.7 is the current waveform of phase A and the converted GAF image when T_1 and T_2 tubes have an open-circuit fault at 0.20 s.

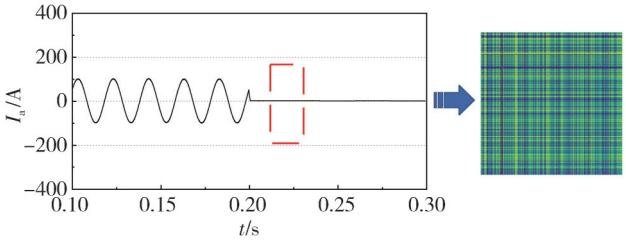

Fig. 7 A-phase current waveform and GAF image of T_1 and T_2 tubes with open-circuit fault

In the simulation model of Matlab/Simulink, 22 working states were simulated respectively, and the A-phase current data under different working states were obtained and then converted into corresponding 2D GAF images. The current signal is equally divided into the different subsections according to the time interval of a period of 0.02 s in the power frequency alternating current, and each subsection corresponds to a GAF image. The A-phase current signal obtained in each working state is divided into 500 small segments, that is, 500 feature maps are determined, and a total of 11 000 feature maps are obtained for 22 working states. In reality, the signal data collected by the sensor are always accompanied by noise. In order to verify the ability of this method to withstand noise interference, the white Gaussian noises with signal-to-noise ratios of 20 dB, 30 dB and 40 dB respectively are superimposed on the current signal output by the model, so that the output signal is closer to reality. Therefore, this experiment generates a total of 44 000 feature maps in 4 groups. Finally, it is divided into training set and test set according to the ratio of 7 ∶ 3. The converted GAF images of the current data of the inverter in 22 working states are shown in Fig. 8(a) Normal, (b) Single IGBT fault, (c) Two-IGBT fault in the same phase bridge arm, (d) Two-IGBTs fault in the same half bridge, and (e) Two-IGBT fault in the cross bridge arm.

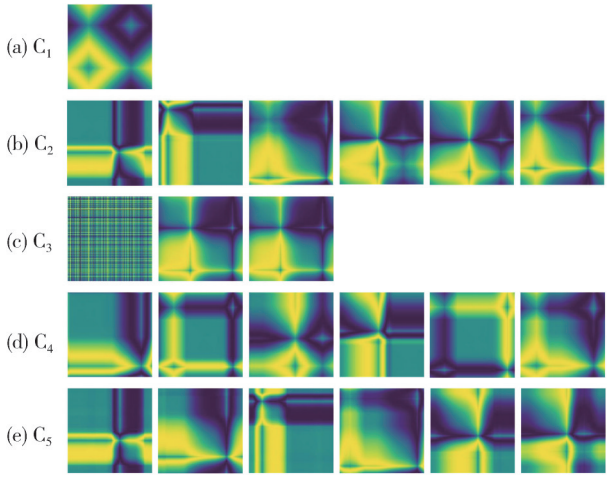

Fig. 8 GAF images of inverter under 22 working states

According to the GAF principle introduced in the first section, the GAF images show the changing trend of the time series from the upper left to the lower right. When the amplitude of the fault signal changes slowly, a large connected area with similar colors will appear in the corresponding GAF image, while the amplitude of the fault signal changes greatly in a short time, a horizontal or vertical line will appear.

4.3 Analysis of training results

The construction platform of the algorithm model in this study is TensorFlow-GPU version 2.5.0, the compiled language is Python 3.9, and the operating environment is Pycharm. The computer hardware is AMD R7 CPU, RTX3050ti GPU, and the system is Win11.

The figures below show the accuracy and loss rate curves trained using the CNN model introduced in Section 2.2. Fig.9 and Fig.10 show the accuracy and loss rate curves without superimposed white Gaussian noise (Noise free). It can be seen that the recognition accuracy and loss rate of the training set tend to be stable after 40 iterations of training, and the final recognition accuracy reaches 100%. The recognition accuracy of the test set fluctuates greatly before 60 iterations of training, stabilizes at more than 98.21% after 60 iterations, and basically reaches more than 99.95% after 80 iterations of training. Finally, at the end of 100 iterations of training, the recognition accuracy rate is

99.99%.

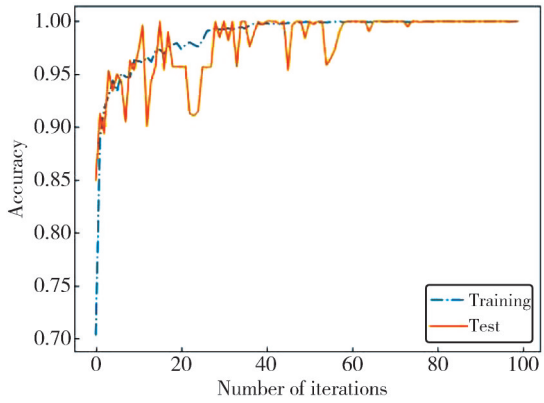

Fig. 9 Accuracy curve(noise free)

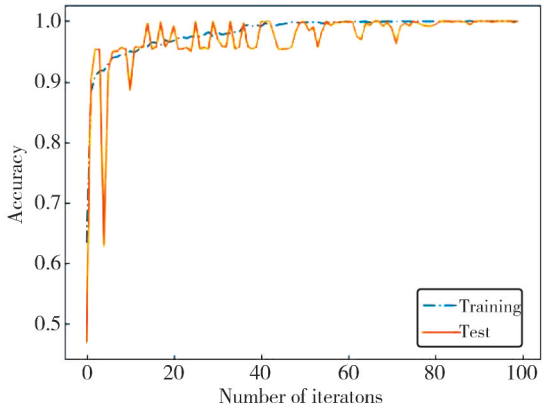

Fig. 10 Loss rate curve(noise free)

Fig.11 and Fig.12 show the curves of accuracy and loss rate when white Gaussian noise is superimposed (SNR=20 dB).

It can be seen that the recognition accuracy and loss rate of the training set are basically the same as those without superimposed white Gaussian noise. The recognition accuracy of the test set fluctuates greatly before 80 iterations of training, and stabilizes at more than 98.24% after 80 iterations. Finally, at the end of 100 iterations of training, the recognition accuracy is 99.36%. Therefore, we can conclude that the GAF-CNN as inverter fault diagnosis method has better anti-noise interference ability.

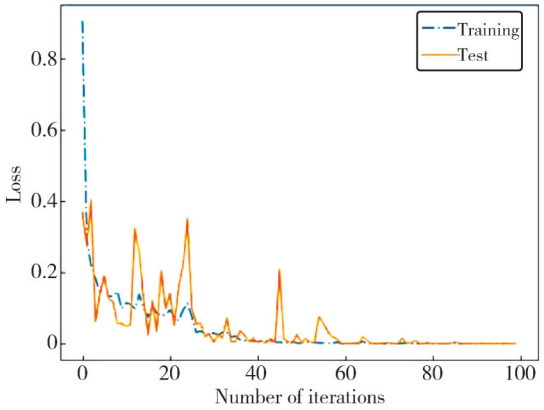

Fig. 11 Accuracy curve(SNR=20 dB)

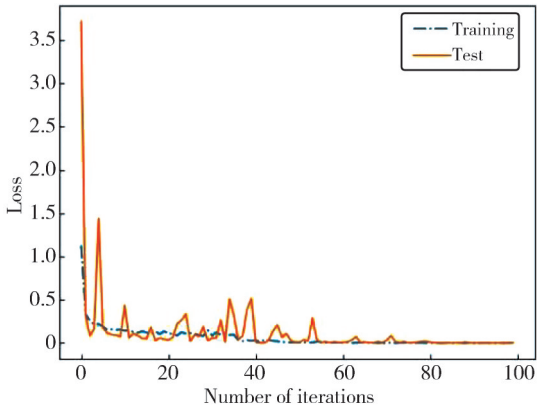

Fig. 12 Loss rate curve(SNR=20 dB)

Table 3 shows the recognition accuracy of the test set under different iterations when the fault signal is superimposed with 20 dB, 30 dB, and 40 dB white Gaussian noise and without white Gaussian noise. From Table 3, it can be seen that the GAF-CNN adopted in this study has a high recognition accuracy of the fault current signal of the inverter, reaching more than 99.36%. It is less affected by noise, and has strong ability to carry noise interference and strong robustness.

Table 3 Recognition accuracy under different noises superimposed

Iterations	Recognition accuracy/%			
	Noise free	SNR=20 dB	SNR=30 dB	SNR=40 dB
20	96.22	95.21	95.98	96.21
40	97.46	95.65	96.14	96.33
60	98.21	96.46	96.97	97.08
80	99.95	98.24	98.60	98.57
100	99.99	99.36	99.52	99.74

4.4 Comparative analysis

In order to verify the advancement and superiority of the method in this paper, the GAF-CNN algorithm is compared with the three intelligent fault diagnosis algorithms mentioned in Ref. [21]. The three methods are wavelet transform (WT) combined with back propagation (BP) neural network, WT combined with support vector machine (SVM), and compressed sensing (CS) combined with SVM. The comparison results of fault diagnosis effects are shown in Table 4.

It can be seen that the diagnostic time of GAF-CNN is 0.134 s. The diagnostic time is composed of the current signal sampling time, the transform time of 1D times series to 2D image, and the diagnostic time. Among them, the fault current signal sampling time is 0.02—0.04 s, that is, the time to sample 1—2 current cycle signal data, the average time converting 1D times series to 2D image is 0.008 6 s, and the average diagnostic time is 0.095 s. Thus, the total average time is 0.134 s. Therefore, compared with

the traditional SVM method, the GAF-CNN improves the fault diagnosis accuracy and fault diagnosis rate.

Table 4 Comparison of different fault diagnosis methods

Diagnostic method	Average fault diagnostic accuracy/%	Mean time for fault diagnosis/s
WT combined with BP neural network[20]	87.50	16.680
WT combined with SVM[20]	94.45	1.180
CS combined with SVM[20]	98.79	0.158
GAF-CNN	99.36	0.134

5 Conclusions

In order to give full play to the advantages of deep learning in recognizing 2D images, we propose a new inverter fault diagnosis method, which uses GAF-CNN model to achieve the detection, classification and localization of inverter fault. Furthermore, the reliability and effectiveness of this method are verified by simulation. The results show that the GAF-CNN can well distinguish the different working states of the inverter IGBT, and then complete the fault diagnosis, classification and localization. With the increase of data samples during inverter operation, the diagnostic accuracy and diagnostic rate of the model can be further improved. Compared with other methods, it has better performance in terms of recognition accuracy and noise immunity. To sum up, the inverter fault diagnosis method based on GAF-CNN has certain value in practical applications.

Acknowledgement

I would like to express my gratitude to the reviewers and editors.

Declaration of conflicting interests

The authors have no conflict of interests related to this publication.

References

[1] ZHANG L, SUN K, XING Y, et al. A family of five-level dual-buck full-bridge inverters for grid-tied applications. IEEE Transactions on Power Electronics, 2016, 31(10): 7029-7042.

[2] FANG Y, JIA K, YANG Z, et al. Impact of inverter-interfaced renewable energy generators on distance protection and an improved scheme. IEEE Transactions on Industrial Electronics, 2019, 66(9): 7078-7088.

[3] WU X, TIAN R, CHENG S, et al. A nonintrusive diagnostic method for open-circuit faults of locomotive inverters based on output current trajectory. IEEE Transactions on Power Electronics, 2018, 33(5): 4328-4341.

[4] GENG Y W, LI W, WANG K. Fault diagnosis method for three-phase photovoltaic grid-connected inverter. Transactions of China Electrotechnical Society, 2014, 29(S1): 203-209.

[5] HAN S, ZHOU M, ZHENG S Q. Open-circuit fault diagnosis of three-phase voltage source inverter based on BP neural network. Journal of Henan Polytechnic University (Natural Science), 2021, 40(6): 126-131.

[6] ZHAO H, XU H R, MEI Z G, et al. Fault diagnostic system for inverter open-circuit faults based on neural network. Power Electronics, 2021, 55(2): 45-49.

[7] ZHU Q Y, LIU W L, TAN X T, et al. Composite fault diagnosis for three-level inverter based on time domain signal. Measurement & Control Technology, 2018, 37(11): 5-10.

[8] SHANG W J, HE Z Y, HU H T, et al. An IGBT output power-based diagnosis of open-circuit fault in inverter. Power System Technology, 2013, 37(4): 1140-1145.

[9] PENG W F, HUANG S R. Study on fault diagnosis of inverters in PMSM drive system. Acta Energiae Solaris Sinica, 2019, 40(7): 1965-1971.

[10] AN Q T, SUN L, ZHAO K, et al. Diagnosis method for inverter open-circuit fault based on switching function model. Proceedings of the CSEE, 2010, 30(6): 1-6.

[11] XU L J. Research on grid inverter fault diagnosis based on bond graph and the BP neural network. Urumqi: Xinjiang University, 2015.

[12] ZHOU F Y, JIN L P, DONG J. Review of convolutional neural network. Chinese Journal of Computers, 2017, 40(6): 1229-1251.

[13] LI G, LI J, GUO Q, et al. Fault diagnosis method of three-phase inverter based on time convolutional neural network. Recent Advances in Electrical & Electronic Engineering, 2022, 15(5): 401-409

[15] WU Y A, YANG F, LIU Y, et al. A comparison of 1-D and 2-D deep convolutional neural networks in ECG classification//IEEE Engineering in Medicine and Biology Society, July 17-21, 2018, Hawaii, USA. New York: IEEE, 2018: 323-327.

[16] YANG S, LUO X, LI C. Fault diagnosis of rotation vector reducer for industrial robot based on a convolutional neural network. Strojniški Vestnik—Journal of Mechanical Engineering, 2021, 67(10): 489-500.

[17] XIAO X, XIAO Y X, ZHANG Y J, et al. Research on the application of the data augmentation method based on 2D gray pixel images in the fault diagnosis of motor bearing. Proceedings of the SEE, 2021, 41(2): 738-749.

[18] WANG Y F, A K X, LIU K W, et al. Research on fault diagnosis method of switch machine based on deep learning. Journal of Test and Measurement Technology, 2023, 37

(2): 106-111.
[19] ZHOU Z C, LIU K, JIANG J F, et al. Distributed optical fiber densing intrusion pattern recognition based on GAF and CNN. Journal of Lightwave Technology, 2020, 38(15): 4174-4182.
[20] ZHAO D Y, DONG W G, GAO F Y. Improved inverter fault diagnosis based on convolutional neural network. Journal of Power Supply, 2020, 18(3): 124-132.
[21] CHENG Y Q. Rescarch on fault diagnosis of tranction inverter based on compressed sensing theory. Lanzhou: Lanzhou Jiaotong University, 2020.

基于GAF-CNN的三相逆变器故障诊断

董唯光，陆浩博*，李生昌

兰州交通大学 自动化与电气工程学院，甘肃 兰州 730070

摘　要： 为了将深度学习在识别二维图像上的优势应用于三相逆变器故障诊断，提出了一种格拉姆角场（Gramian angular field，GAF）结合卷积神经网络（Convolutional neural network，CNN）的三相逆变器故障诊断模型。由于逆变器不同工作状态时的电流信号不同，其时间序列编码形成的图像也不同，因此，图像识别技术可用于时间序列分类，以识别逆变器故障电流信号。首先，将一维的逆变器故障电流信号通过GAF转化为二维图。其次，输入构造的适合逆变器故障诊断的CNN模型，实现对逆变器故障的检测、分类和定位。仿真结果表明，该方法在不同的噪声数据下，识别准确率均高于99.36%，较其他传统方法具有更高的准确性和可靠性、更强的抗噪声干扰能力和鲁棒性，是一种行之有效的逆变器故障诊断方法。

关键词： 故障诊断；格拉姆角场；卷积神经网络；抗噪声干扰；鲁棒性

引用格式： DONG Weiguang, LU Haobo, LI Shengchang. Fault diagnosis of three-phase inverter based on GAF-CNN. Journal of Measurement Science and Instrumentation, 2025, 16(3): 456-463. DOI: 10.62756/jmsi.1674-8042.2025044